Stark Spectroscopy on the LH2 Complex from *Rhodobacter sphaeroides* Strain G1C; Frequency and Temperature Dependence†

Kazuhiro Yanagi and Hideki Hashimoto*

"Light and Control", PRESTO/JST and Department of Physics, Graduate School of Science, Osaka City University, 3-3-138 Sugimoto, Sumiyoshi-ku, Osaka 558-8585, Japan

Alastair T. Gardiner and Richard J. Cogdell*

Institute of Biomedical and Life Sciences, Division of Biochemistry and Molecular Biology, University of Glasgow, Glasgow G12 8QQ, Scotland, U.K.

Received: December 14, 2003; In Final Form: March 17, 2004

Electroabsorption (Stark effect) spectroscopy using dual-phase lock-in detection was applied to the B850 absorption band of the peripheral antenna (LH2) complex from the purple non-sulfur bacterium *Rhodobacter sphaeroides* strain G1C. Electroabsorption signals due to the electrostatic interaction between pigments and surrounding apoproteins were clearly detected from the phase-retarded signal. The temperature and frequency dependence of the phase-retarded signal were used to gain insights on the dynamics of the pigment−protein interactions.

Introduction

It is a great pleasure to contribute this paper in honor of Gerry Small, who performed a large number of influential studies on photosynthetic pigment−protein complexes. We are very pleased, therefore, to present this paper on one of the light-harvesting complexes with which Gerry has been so strongly associated.

Stark spectroscopy is a useful technique with which to probe the pigment−pigment and pigment−protein interactions in photosynthetic pigment−protein complexes. For an excellent review in this area interested readers should consult Boxer (1993).[1] Although the general theory behind the Stark shift is relatively well developed, a better theoretical understanding of Stark spectroscopy in a biological context is required. This is needed to be able to correlate details of the measured spectra with a structural understanding of the pigment interactions, and how these affect the magnitude of the experimentally determined Stark shifts. In this study Stark spectra of the LH2 complex from the purple non-sulfur photosynthetic bacterium *Rhodobacter (Rb.) sphaeroides* strain G1C were investigated with special emphasis on the effects of temperature and the frequency of the applied electric field.

Most previous reports on the use of Stark spectroscopy to study photosynthetic pigment−protein complexes have only used in-phase signals.[2−18] Although these studies have been very informative, more detailed information on dynamic electrostatic interactions with the environment can be obtained from the out-of-phase (quadrature-phase) signal. When a pigment is subjected to an electric field and shows a Stark shift, the quadrature-phase signal depends on the pigment's interaction with the surrounding environment. By studying the frequency and temperature dependence of the quadrature-phase signals the nature of this interaction can be investigated. Stark spectra of the J-aggregates of a pseudo-isocyanine dye (1,1′-diethyl-2,−2,2′-quinocyanine bromide) showed the first, clear evidence of the presence of the quadrature-phase signal.[19,20] The Stark shift was sensitive to the change in the relative geometrical configuration between the cationic dyes and the surrounding anionic environment. The reason for the appearance of this phase retarded signal was interpreted as being due to displacement of the anions surrounding these J-aggregates. In the case of the LH2 complex from *Rb. sphaeroides* we set out to investigate whether this approach, together with our knowledge of the structure of LH2 complexes, could be used to identify components of the interactions responsible for the quadrature-phase signal. At the outset, it was expected that polar amino acid residues would dominate electrostatic interactions with the pigments. The outcome of this expectation is discussed below.

Methods

Complex Purification. Cells of *Rb. sphaeroides* strain G1C were grown photosynthetically in the light and harvested by centrifugation. The cells were then disrupted and chromatophores prepared essentially as described in Cogdell and Crofts (1978).[21] Chromatophores were then adjusted to an NIR $OD_{850} = 50$ with 20 mM Tris·HCl (pH8.0) and solubilized with 1.0% (v/v) lauryldimethylamine *N*-oxide (LDAO) for 1 h at 26 °C. After any unsolubilized material had been removed by centrifugation the LH2 complex was purified sequentially by ion-exchange (DE52, Whatman) chromatography and (S-200 Superdex, Amersham Bioscience) gel filtration chromatography. The quality of the final, purified LH2 complex was checked spectrophotometrically and had a purity ratio (OD_{850}/OD_{280}) of 2.7, concentrated, aliquoted, and frozen until required.

Optical Characterization. LH2 complexes were dispersed isotropically in poly(vinyl alcohol) (PVA) films (PVA-217, Kuraray Co., Ltd.) and electroabsorption (EA) and optical absorption spectra recorded. These films were prepared according to the following procedure. Both the LH2 complexes

† Part of the special issue "Gerald Small Festschrift".

* Corresponding authors. H.H.: phone & fax, +81-6-6605-2526; e-mail, hassy@sci.osaka-cu.ac.jp. R.J.C.: phone, +44-141-330-4332; fax, +44-141-330-4620; e-mail, R.Cogdell@bio.gla.ac.uk.

10.1021/jp037863+ CCC: $27.50
Published on Web 05/05/2004

($OD_{850} = 5$) and the PVA polymer (1%) were dissolved into a buffer solution (20 mM Tris·HCl, 0.05% (v/v) LDAO, pH 8.0). A small aliquot of this solution was then dropped upon the surface of a glass substrate, on which gold electrodes (gap distance is 50−100 μm) had been installed. The gap distance between the electrodes was determined by optical microscopy to an accuracy of 2 μm. Any residual solvent was then removed under reduced pressure. The optical absorption spectra were recorded using a UV/vis spectrophotometer (JASCO, V-530). EA spectra were recorded in the setup described below.[22,23] Light from a 150 W tungsten−halogen lamp (Mejiro Precision Co., PHL-150) was dispersed by a monochromator (Acton Research, SpectraPro 150) and used to irradiate the sample cell. The incident radiation was linearly polarized using a Glan-Thompson prism and guided to the gap between the electrodes on the sample cell. The angle between the electric vector of the incident light and the electric field applied to the sample was set at 54.7° (magic angle). Unless otherwise stated a sinusoidal ac voltage with a frequency $f = 500$ Hz generated by a function generator (NF, E-1201A) was amplified to a high voltage (40 kV/cm) with a high-voltage bipolar amplifier (NF, 4305). The intensity of the light transmitted through the sample was detected using a silicon photodiode (Hamamatsu, S1336-8BQ). The dc component of the signal was recorded on a digital multimeter (Fluke, 45), whereas the ac component was amplified using a dual-phase lock-in amplifier (NF, 5610B). Among the changes (ΔI) of the transmitted light intensity (I) induced by the applied electric field with frequency f, only those with $2f$ frequency were selectively amplified by the lock-in amplifier. Absorbance changes (ΔA) induced by the applied electric field were then calculated by using the following equation, $\Delta A = -\ln[(I + \Delta I)/I]/2.303$. The temperature dependence of the EA spectra was studied by using a temperature-controlled liquid-nitrogen cryostat (Oxford, Optistat-DN). The sample temperature was regulated between 79 and 293 K with an accuracy of ±0.1 K. Applied electric field frequency dependence of the EA spectra was studied in the frequency range between 20 and 1000 Hz at room temperature.

Theory of Dual-Phase Lock-in Detection. When the orientation effect and the change of transition dipole moments upon exposure of the externally applied electric field are ignored, the absorption change (ΔA) due to the applied electric field can be written as the first- and second-order derivatives of the absorption spectra (A),[24−28]

$$\Delta A = \left\langle \frac{(\Delta\mu\cdot\mathbf{E})}{h}\nu\frac{\partial A/\nu}{\partial\nu} + \frac{1}{2}\frac{\mathbf{E}:\Delta\alpha:\mathbf{E}}{h}\nu\frac{\partial A/\nu}{\partial\nu} + \frac{1}{2}\frac{(\Delta\mu\cdot\mathbf{E})^2}{h^2}\nu\frac{\partial^2 A/\nu}{\partial\nu^2}\right\rangle \quad (1)$$

Here, $\Delta\mu$ is the dipole moment change upon photoexcitation, and $\Delta\alpha$ is the change in the polarizability upon photoexcitation. Averaging over the whole ensemble of sample orientations, i.e., over their $\Delta\mu$ and $\Delta\alpha$ distributions, is represented by a pair of brackets, $\langle\ \rangle$.

The change in dipole moment of a pigment surrounded by an apoprotein is caused by two different effects.[27] The first is due to $\Delta\mu_{mol}$, which corresponds to the intrinsic $\Delta\mu$ of the pigment. The other is due to $\Delta\mu_{pocket}$, which arises from the internal electric field of the apoprotein mediated by $\Delta\alpha$ of the pigment. This internal electric field is termed the pocket field, $\mathbf{E}_{pocket}$. Therefore, $\Delta\mu$ can be written as[27]

$$\Delta\mu = \Delta\mu_{mol} + \Delta\alpha:\mathbf{E}_{pocket} = \Delta\mu_{mol} + \Delta\mu_{pocket} \quad (2)$$

The pocket field strength depends on the position of polar amino acid residues. Therefore, the pocket field can be described as a function of the displacement parameter, $\mathbf{x}$, of such an amino acid residue from its equilibrium position by means of a Taylor expansion,

$$\mathbf{E}_{pocket}(\mathbf{x}) = \mathbf{E}_{pocket}(\mathbf{0}) + [\nabla\cdot\mathbf{E}_{pocket}(\mathbf{0})]\cdot\mathbf{x} = \mathbf{E}_{pocket}(\mathbf{0}) + C\cdot\mathbf{x} \quad (3)$$

It is assumed that the externally applied electric field can modulate the position of this polar amino acid residue. The displacement factor, $\mathbf{x}$, is then related to the externally applied electric field through the following equation of damping oscillator,[29]

$$\frac{d^2\mathbf{x}}{dt^2} = -\gamma\frac{d\mathbf{x}}{dt} - \omega_0{}^2\mathbf{x} + \frac{q\cdot\mathbf{E}}{m} \quad (4)$$

Here, γ is a relaxation factor that reflects a dynamic protein environment around the amino acid residue and ω_0 is its resonance frequency. The charge and mass of the amino acid residue are given by q and m, respectively. When a sinusoidal electric field is applied with frequency ω, $\mathbf{E}(t) = f_L\cdot\mathbf{E}_{ext}\sin(\omega t)$ (here f_L is a local-field correction factor), eq 4 can be solved and the displacement parameter, $\mathbf{x}(t)$, can be written as

$$\mathbf{x}(t) = \frac{q}{m}\frac{f_L\cdot\mathbf{E}_{ext}}{((\omega_0{}^2 - \omega^2)^2 + \gamma^2\omega^2)^{1/2}}\sin(\omega t - \phi) = x_0\cdot f_L\cdot\mathbf{E}_{ext}\sin(\omega t - \phi) \quad (5)$$

$$x_0 = \frac{q}{m}\frac{1}{\sqrt{(\omega_0{}^2 - \omega^2)^2 + \gamma^2\omega^2}} \quad (6)$$

$$\tan\phi = \frac{\gamma\omega}{\omega_0{}^2 - \omega^2} \quad (7)$$

Equation 5 indicates that the displacement parameter follows the applied electric field with a phase delay ϕ. This phase-retarded component is due to the presence of the relaxation factor γ. From eqs 2, 3, and 5, the first term of eq 1 can be written as

$$\left\langle \frac{(\Delta\mu\cdot\mathbf{E})}{h}\nu\frac{\partial A/\nu}{\partial\nu}\right\rangle = \frac{x_0 C}{3h}\Delta\alpha\cdot f_L{}^2 E_{ext}{}^2\sin(\omega t)\sin(\omega t - \phi)\cdot\nu\frac{\partial A/\nu}{\partial\nu} \quad (8)$$

The second and the third terms in eq 1 can be written as

$$\left\langle \frac{1}{2}\frac{\mathbf{E}:\Delta\alpha:\mathbf{E}}{h}\nu\frac{\partial A/\nu}{\partial\nu}\right\rangle = \frac{1}{6h}\Delta\alpha\cdot f_L{}^2 E_{ext}{}^2\sin^2(\omega t)\cdot\nu\frac{\partial A/\nu}{\partial\nu} \quad (9)$$

and

$$\left\langle \frac{1}{2}\frac{(\Delta\mu\cdot\mathbf{E})^2}{h^2}\nu\frac{\partial^2 A/\nu}{\partial\nu^2}\right\rangle = \left(\frac{1}{6h^2}(\Delta\mu^*)^2\cdot f_L{}^2 E_{ext}{}^2\sin^2(\omega t) + \frac{x_0{}^2 C^2\Delta\alpha^2\cdot f_L{}^4 E_{ext}{}^4\sin^2(\omega t)\sin^2(\omega t - \phi)}{10h^2}\right)\cdot\nu\frac{\partial^2 A/\nu}{\partial\nu^2} \approx \frac{1}{6h^2}(\Delta\mu^*)^2\cdot f_L{}^2 E_{ext}{}^2\sin^2(\omega t)\cdot\nu\frac{\partial^2 A/\nu}{\partial\nu^2} \quad (10)$$

$$\Delta\mu^* = \Delta\mu_{mol} + \Delta\alpha:\mathbf{E}_{pocket}(\mathbf{0}) \quad (11)$$

In eq 10, the quadratic term of C is neglected. Finally, the absorption change modulating with 2ω frequency, $\Delta A_{2\omega}$, upon exposure of the sinusoidal electric field with frequency ω can be written as

$$\Delta A_{2\omega} = \frac{x_0 C}{3h}\Delta\alpha\cdot\nu\frac{\partial A/\nu}{\partial\nu}\frac{{f_L}^2{E_{ext}}^2\cos(2\omega t-\phi)}{2} + \frac{1}{6}\left(\frac{\Delta\alpha}{h}\nu\frac{\partial A/\nu}{\partial\nu}+\frac{\Delta\mu^{*2}}{h^2}\nu\frac{\partial^2 A/\nu}{\partial\nu^2}\right)\frac{{f_L}^2{E_{ext}}^2\cos(2\omega t)}{2} \quad (12)$$

From this it can be seen that there are two contributions to this absorption change: an ordinal term that follows the externally applied electric field without delay and a phase-retarded term that follows with a phase delay, ϕ. The two contributions can be decomposed into in-phase and quadrature-phase components by means of dual-phase lock-in detection of the EA signals. When the reference signal of a lock-in amplifier is set as $F_{ref} = F_0\cos(2\omega t)$, in-phase ($\Delta A_{in}$) and quadrature-phase ($\Delta A_{quad}$) signals detected in a dual phase lock-in amplifier can be written as

$$\Delta A_{in} = \frac{1}{6}\left[\left(\frac{\Delta\alpha}{h}+\frac{2x_0\cdot C\cdot\Delta\alpha}{h}\cos\phi\right)\cdot\nu\frac{\partial A/\nu}{\partial\nu}+(\Delta\mu^*)^2\nu\frac{\partial^2 A/\nu}{h^2\partial\nu^2}\right]\cdot\frac{{f_L}^2\cdot{E_{ext}}^2}{2}$$

$$= \frac{1}{6}\left(F_{in}\cdot\nu\frac{\partial A/\nu}{h\partial\nu}+(\Delta\mu^*)^2\nu\frac{\partial^2 A/\nu}{h^2\partial\nu^2}\right)\cdot\frac{{f_L}^2\cdot{E_{ext}}^2}{2} \quad (13)$$

$$F_{in} = \Delta\alpha\cdot(1+2x_0\cdot C\cos\phi) = \Delta\alpha\cdot\left(1+2\frac{qC}{m}\frac{(\omega_0{}^2-\omega^2)}{(\omega_0{}^2-\omega^2)^2+\gamma^2\omega^2}\right) \quad (14)$$

and

$$\Delta A_{quad} = \frac{1}{6}(2x_0\cdot C\cdot\Delta\alpha\sin\phi)\cdot\nu\frac{\partial A/\nu}{h\partial\nu}\cdot\frac{{f_L}^2\cdot{E_{ext}}^2}{2} = \frac{1}{6}F_{quad}\cdot\nu\frac{\partial A/\nu}{h\partial\nu}\cdot\frac{{f_L}^2\cdot{E_{ext}}^2}{2} \quad (15)$$

$$F_{quad} = 2x_0\cdot C\cdot\Delta\alpha\sin\phi = 2\Delta\alpha\frac{qC}{m}\frac{\gamma\omega}{(\omega_0{}^2-\omega^2)^2+\gamma^2\omega^2} \quad (16)$$

Equations 13 and 15 indicate that for in-phase spectra, first- and second-order derivative waveforms of absorption spectra can be observed; however, in quadrature-phase spectra, only the first-order derivative form can be detected. The quadrature-phase signals only arise from the phase-retarded component. Thus, if there is not a strong electrostatic interaction between a pigment and an amino acid residue, i.e., the protein environment, this phase-retarded signal will not be observed. Simple misalignment of the lock-in amplifier phase did not produce a first-derivative waveform in the quadrature-phase EA signal but rather gave rise to a waveform spectrum similar to that of the in-phase. The phase-retarded component of the quadrature-phase EA signal is diagnostic for the presence of an electrostatic interaction between the pigments and the polar amino acid residues.

Results and Discussion

Absorption and Electroabsorption Spectroscopy of the LH2 Complex from *Rb. sphaeroides* G1C. Figure 1a shows a typical absorption spectrum of the LH2 complex from *Rb. sphaeroides* strain G1C. The crystal structure of the homologous LH2 complex from *Rhodopseudomonas (Rps.) acidophila* strain 10050[30−32] has been determined to a resolution of 2.0 Å. The light-absorbing pigments bacteriochlophyll (Bchl) and carotenoids are noncovalently bound to two heterologous low-molecular weight hydrophobic apoproteins termed α and β. Bchl molecules in this complex are divided into two spectral forms: monomeric Bchl that has a Q_y absorption band at 800 nm (B800) and strongly exciton coupled molecules that have a Q_y absorption band at 850 nm (B850). The B800 Bchl molecules are a group of nine monomers separated center-to-center by about 21 Å. The central Mg^{2+} ions of these Bchls are liganded to an extension of the *N*-terminal methionine residue of the α-apoprotein. The B850 absorption band results from a ring of eighteen strongly interacting, overlapping Bchl molecules, in which the central Mg^{2+} ions are liganded to conserved histidine residues. Bchl also has two additional absorption bands: the Q_x band at 590 nm and the Soret (or B) band at 380 nm. The carotenoid present, in a twisted all-trans configuration, in the G1C complex is neurosporene. It exhibits three strong absorption peaks in the 440−540 nm region and efficient energy transfer from carotenoid to Bchl indicates that the π−electron system in the two pigment types must be in van der Waals contact.

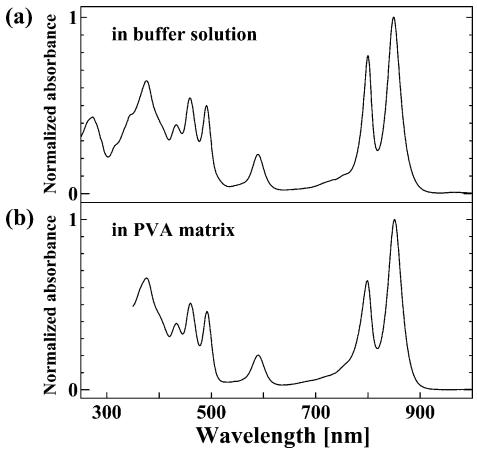

Figure 1. Absorption spectra of the LH2 complex normalized at 850 nm from *Rb. sphaeroides* G1C (a) in buffer solution (20 mM Tris·HCl, 0.05% (v/v) LDAO, pH 8.0) and (b) in PVA matrix on BK7 glass substrate recorded at room temperature. Absorption data below 350 nm of the PVA matrix is omitted because of the poor transmission of light through the BK7 glass substrate.

Figure 1b compares the absorption spectrum of the LH2 complex from *Rb. sphaeroides* G1C in a PVA matrix with that of the complex in buffer. The spectra show that when the LH2 complex is incorporated into the PVA matrix a small fraction of the B800 absorption is lost. This is, however, a relatively small change. Equation 12 shows that $\Delta\alpha$ and $\Delta\mu$ values can be derived from the coefficients of the first- and second-order derivatives of absorption spectra. However, it is important to recognize that this equation implicitly assumes uniform nonlinearity over an entire absorption band. If this assumption is not valid, as sometimes happens when an absorption band is composed of several subbands, a deconvolution protocol is required to determine the nonlinear optical parameters of each subband.[22,33] Because the higher order vibronic transitions of the lower energy band overlap in the spectral region of the B800 and the carotenoid absorption bands are complex, it is not straightforward to evaluate the nonlinear optical properties of these bands from their EA spectra. To circumvent these

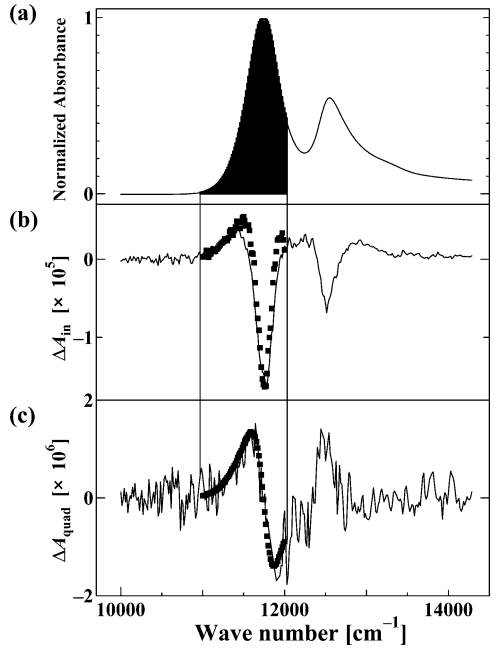

Figure 2. (a) Normalized absorption spectrum as well as (b) in-phase and (c) quadrature-phase electroabsorption spectra of the LH2 complex from *Rb. sphaeroides* strain G1C dispersed in PVA polymer films at room temperature. Spectral data were analyzed concentrating on the 11000−12000 cm^{-1} spectral region (B850 absorption band), which is marked with shadow in the absorption spectrum. Solid squares in (b) and (c) show the results of spectral simulation. Note that the second-order derivative type waveform is observed in the in-phase electroabsorption spectrum, whereas only the first-order derivative waveform is observed in the quadrature-phase.

problems and because of the small loss of absorption in the B800 region, this study has concentrated on the lowest energy B850 band.

Figure 2 shows absorption (a), in-phase (b), and quadrature-phase (c) EA spectra of the LH2 complex focusing on the B850 band. The spectral form in the quadrature phase is completely different from that obtained with the in-phase signal. The in-phase spectrum resembles the second-order derivative of the absorption spectrum, whereas the quadrature-phase spectrum resembles its first-order derivative. Quadrature-phase signals can also be obtained when the phase of the EA signals do not match those of the reference signals. However, in such a case, the spectral form of the quadrature-phase signal must be the same as that of the in-phase signal (vide supra). The observed spectral difference between the two phases clearly indicates that this phase-retarded signal arises from another mechanism.

We assume that the phase-retarded signals result from a strong electrostatic interaction between pigments and apoprotein. Our physical model, described in a previous section, predicts that phase-retarded signals should be observed in the quadrature-phase upon application of EA spectroscopy with dual phase lock-in detection and that the spectral form of this phase will be completely different from that detected in the in-phase signal. As described in eqs 13 and 15, the in-phase EA spectrum should be a linear combination of the first- and second-order derivatives, whereas the quadrature-phase EA spectrum should only be the first-order derivative of the original absorption spectrum of the B850 band. The observed EA spectra of the B850 band could be satisfactorily reproduced, by this curve fitting procedure (waveform analysis), as illustrated in Figure 2 (square symbols). The temperature and frequency dependence of these signals were investigated to identify the physical origin of the phase-retarded components.

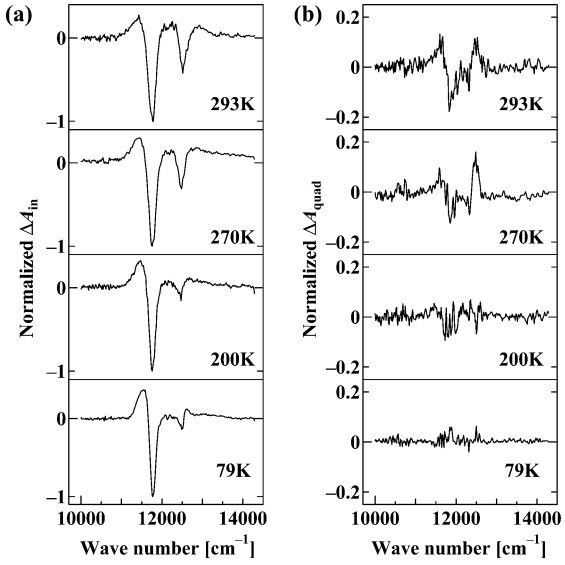

Figure 3. (a) In-phase and (b) quadrature-phase electroabsorption spectra of the LH2 complex from *Rb. sphaeroides* strain G1C dispersed in PVA polymer films at 293, 270, 200, and 79 K. Data are again shown with regard to the spectral region of the B850 absorption band. The spectral data were normalized at 11771 cm^{-1} of the in-phase signal at each temperature.

Temperature Dependence of the Phase-Retarded Signals. Equation 7 indicates that the phase-retarded signals are due to the relaxation factor, γ. This physical quantity is the inverse of the relaxation time, t_r, which is often used to characterize viscoelastic behavior of polymer molecules.[34] Because the temperature dependence of the relaxation time usually yields an Arrhenius form, the temperature dependence of γ can be described as

$$\gamma \propto \frac{1}{t_r} \propto \exp\left(-\frac{H}{RT}\right) \tag{17}$$

Here H is the activation energy that characterizes the relaxation factor. According to our model, F_{quad} can be written as

$$F_{quad} = 2\Delta\alpha\frac{qC}{m}\frac{\gamma\omega}{(\omega_0{}^2 - \omega^2)^2 + \gamma^2\omega^2} \propto \gamma\Delta\alpha \tag{18}$$

Therefore, it is predicted that as temperature decreases the phase-retarded signals will disappear. Figure 3 shows the temperature dependence of (a) the in-phase and (b) the quadrature-phase EA spectra. The phase-retarded signals, which are clearly observed at room temperature, disappear at 79 K just as our model predicts. The $\Delta\alpha$ and $\Delta\mu^*$ values determined from the waveform analysis of the EA spectrum at 79 K [$\Delta\alpha$ = 580 [$Å^3/f_L{}^2$], $\Delta\mu^*$ = 3.7 [D/f_L]] are consistent with the values of $\Delta\alpha$ and $\Delta\mu$ previously reported for the B850 band in the LH2 complex from *Rb. sphaeroides* 2.4.1 [$\Delta\alpha$ = 619 [$Å^3/f_L{}^2$], $\Delta\mu$ = 4.2 [D/f_L]].[17] These previously reported $\Delta\alpha$ and $\Delta\mu$ values were determined with a similar method of dual-phase lock-in detection as adopted in this study. However, their data set was only recorded at 77 K. On the basis of our present observations, the phase-retarded signals cannot be seen at 77 K. Therefore, this type of phase-retarded signal was probably missed in the previous study. In Figure 3, the intensity of the EA signals in the region of the B800 absorption band also shows a substantial decrease at low temperatures in both the in-phase and quadrature-phase spectra. However, discussion of this about this particular spectral region is beyond the scope of this study due to the reasons already mentioned above.

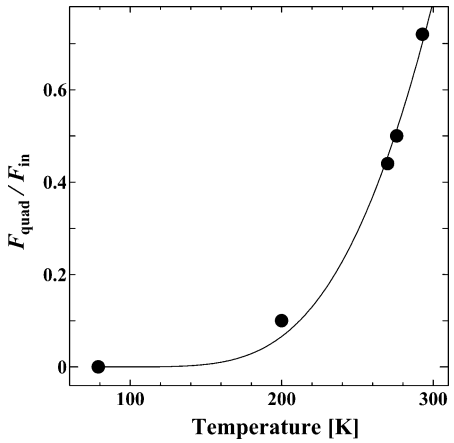

Figure 4. Temperature dependence of the F_{quad}/F_{in} values between 79 and 293 K. Data were collected at 79, 200, 270, 276, and 293 K (closed circles). The solid curve shows the result of fitting using eq 19.

Equation 18 shows that the temperature dependence of $\Delta\alpha$, as well as γ, influences the F_{quad} values. To determine the activation energy, H, it is necessary to investigate the temperature dependence of the relaxation factor γ. According to our model, F_{quad}/F_{in} values are given by the following formula

$$\frac{F_{quad}}{F_{in}} = \gamma \frac{\omega}{\frac{1}{2}\frac{m}{q \cdot C}\cdot[(\omega_0{}^2 - \omega^2)^2 + \gamma^2\omega^2] + \omega_0{}^2 - \omega^2} \propto \exp\left(-\frac{H}{RT}\right) \quad (19)$$

The F_{quad} and F_{in} values were determined by applying waveform analysis to the EA spectra. Figure 4 shows the temperature dependence of F_{quad}/F_{in} values (circles) and the result of a least-squares fitting (solid line). Using eq 19, the activation energy H was determined to be 12 kJ/mol. Quite a number of molecular motions can be possible candidates that generate the relaxation factor, γ, e.g., local mode relaxation, crankshaft and kink motion, rotation of methyl group, side chain motions, local intermolecular rearrangements.[34−36] The activation energy H (=12 kJ/mol), which we have determined in this investigation, lies in the region equivalent to the above molecular motions. However, it is not straightforward to assign which molecular motion can predominate to produce such a small activation energy. Inspection of the X-ray crystal structure of the LH2 complex from *Rps. acidophila* strain 10050, suggests that a plausible candidate for the physical origin of γ could be either a local twisting motion of the apoprotein main chain, or rotational motion of apoprotein side chains. These conclusions are, however, rather general and not unexpected. Future studies using other pigment−protein complexes whose structures are known will be required to get a deeper insight on this particular issue.

Frequency Dependence of the Phase-Retarded Signals. According to eq 16, F_{quad} can be rewritten as a function of the modulation frequency f (=$\omega/2\pi$) of the applied electric field,

$$F_{quad}(f) = 2\Delta\alpha\frac{qC}{m}\frac{2\pi\gamma f}{(\omega_0{}^2 - 4\pi^2 f^2)^2 + 4\pi^2\gamma^2 f^2} \quad (20)$$

Equation 20 includes the term resonance frequency, ω_0. In this context ω_0 corresponds to the kinetic energy of stretching, and/or rotational motions of polar amino acid residues, which have an electrostatic interaction with the chromophore molecules. It is to be expected, therefore, that the origin of the phase-retarded signals can also be deduced from the resonance frequency, ω_0, determined from the frequency dependence of F_{quad}. Figure 5 shows the frequency dependence of F_{quad} (circles) and the result of fitting (solid line) of the data to eq 20. In Figure 5, all the observed F_{quad} values are normalized against F_{quad} at 500 Hz [F_{quad}(500)]. The observed $F_{quad}(f)/F_{quad}$(500) values are well reproduced when ω_0 = 11 kHz. This resonance frequency corresponds well to the rotational motion of aromatic amino acid side chains in the protein.[37,38] Interestingly, the X-ray crystal structure of the LH2 complex from *Rps. acidophila* strain 10050 clearly shows that the Mg^{2+} ions at the center of the B850 bacteriochlorin rings are liganded to histidine side chains. These histidine residues are prime candidates for the strong electrostatic interaction suggested by the presence of the phase-retarded signals. However, the resonance frequency of 11 kHz looks too low for a normal mode reflecting the Mg−His interaction, because the Mg−His stretching mode is reported to be 230−240 cm^{-1} (~1 THz).[39−41] Therefore, we suggest that the relevant normal mode could be an overall, coupled mode reflecting the total local environment of pigment−protein interaction. Isotope effects due to specific ^{13}C and ^{15}N substitutions of key amino acids could provide a powerful way to test this idea.

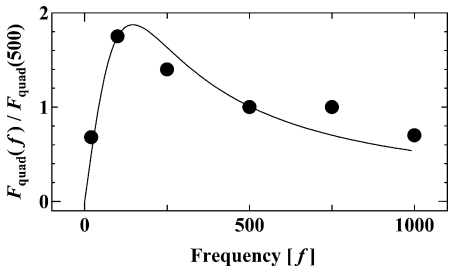

Figure 5. Applied electric field frequency dependence of $F_{quad}(f)/F_{quad}$(500) values between 20 and 1000 Hz. Data collection was performed at f = 20, 100, 250, 500, 750, and 1000 Hz (closed circles). The solid curve shows the result of fitting using eq 20.

Conclusions

Electroabsorption (Stark effect) signals due to electrostatic interactions between the B850 pigments and surrounding apoproteins were detected as a phase-retarded signal using dual-phase lock-in detection. The Arrhenius type activation energy (H = 12 kJ/mol) was determined from the temperature dependence of the phase-retarded signals. The resonance frequency (ω_0 = 11 kHz) was determined from their frequency dependence. The calculated thermodynamic and kinetic parameters can be accounted for by assuming a strong electrostatic interaction of the B850 pigments with the dynamic environment provided by the apoproteins (a local twisting motion of the main chain or rotational motion of the side chains). Further study using other pigment−protein complexes whose structures are known as well as by using specifically isotope substituted pigment−protein complexes should provide a deeper insight into the origins of these electrostatic interactions.

Acknowledgment. H.H. thanks Grant-in-aid from the Japanese Ministry of Education, Culture, Sports, Science & Technology (Grants Nos. 14340090 and 14654072). H.H. and R.J.C. thank the Grant-in-aid from BBSRC and NEDO international joint research. This work is supported in part by the grant from Nakatani Electronic Measuring Technology Association of Japan.

References and Notes

(1) Boxer, S. G. Photosynthetic reaction center spectroscopy and electron-transfer dynamics in applied electric field. In *The Photosynthetic Reaction Center, Volume II*; Deisenhofer, J., Norris, J. R., Eds.; Academic Press: San Diego, 1993; p 179.

(2) Steffen, M. A.; Lao, K.; Boxer, S. G. *Science* **1994**, *264*, 810.

(3) Scherer, P. O. J.; Fischer, S. F. *Chem. Phys. Lett.* **1986**, *153*, 31.

(4) Krawczyk, S.; Krupa, Z.; Maksymiec, W. *Biochim. Biophys. Acta* **1993**, *1143*, 273.

(5) Palacios, M. A.; Frese, R. N.; Gradinaru, C. C.; van Stokkum, I. H. M.; Premvardhan, L. L.; Horton, P.; Ruban, A. V.; Grondelle, R. v.; Amerongen, H. v. *Biochim. Biophys. Acta* **2003**, *1605*, 83.

(6) Middendorf, T. R.; Mazzola, L. T.; Lao, K.; Steffen, M. A.; Boxer, S. G. *Biochim. Biophys. Acta* **1993**, *1143*, 223.

(7) Lösche, M.; Feher, G.; Okamura, M. Y. *Proc. Natl. Acad. Sci. U.S.A.* **1987**, *84*, 7537.

(8) Lockhart, D. J.; Boxer, S. G. *Proc. Natl. Acad. Sci. U.S.A.* **1988**, *85*, 107.

(9) Lockhart, D. J.; Boxer, S. G. *Biochemistry* **1987**, *26*, 664.

(10) Leeuv, D. d.; Malley, M.; Buttermann, G.; Okamura, M. Y.; Feher, G. *Biophys. J.* **1982**, *37*, 111a.

(11) Gottfried, D. S.; Steffen, M. A.; Boxer, S. G. *Science* **1991**, *251*, 662.

(12) Gottfried, D. S.; Steffen, M. A.; Boxer, S. G. *Biochim. Biophys. Acta* **1991**, *1059*, 76.

(13) Gottfried, D. S.; Stocker, J. W.; Boxer, S. G. *Biochim. Biophys. Acta* **1991**, *1059*, 63.

(14) DiMagno, T. J.; Bylina, E. J.; Angerhofer, A.; Youvan, D. C.; Norris, J. R. *Biochemistry* **1990**, *29*, 899.

(15) Braun, H. P.; Michel-Beyerle, M. E.; Breton, J.; Buchanan, S.; Michel, H. *FEBS Lett.* **1987**, *221*, 221.

(16) Boxer, S. G.; Goldstein, R. A.; Lockhart, D. J.; Middendorf, T. R.; Takiff, L. *J. Phys. Chem.* **1989**, *93*, 8280.

(17) Beekman, L. M. P.; Frese, R. N.; Fowler, G. J. S.; Picorel, R.; Cogdell, R. J.; van Stokkum, I. H. M.; Hunter, C. N.; van Grondelle, R. *J. Phys. Chem. B* **1997**, *101*, 7293.

(18) Beekman, L. M. P.; Steffen, M.; Stokkum, I. H. M. v.; Olsen, J. D.; Hunter, C. N.; Boxer, S. G.; Grondelle, R. v. *J. Phys. Chem. B* **1997**, *101*, 7284.

(19) Misawa, K.; Minoshima, K.; Ono, H.; Kobayashi, T. *Chem. Phys. Lett.* **1994**, *220*, 251.

(20) Misawa, K.; Kobayashi, T. *Nonlinear Opt.* **1995**, *14*, 103.

(21) Cogdell, R. J.; Crofts, A. R. *Biochim. Biophys. Acta* **1978**, *502*, 409.

(22) Yanagi, K.; Kobayashi, T.; Hashimoto, H. *Phys. Rev. B* **2003**, *67*, 115122.

(23) Hashimoto, H.; Nakashima, T.; Hattori, K.; Yamada, T.; Mizoguchi, T.; Koyama, Y.; Kobayashi, T. *Pure Appl. Chem.* **1999**, *71*, 2225.

(24) Liptay, W. Dipole moments and polarizabilities of molecules in excited electronic states. In *Excited States*; Lim, E. C., Ed.; Academic: New York, 1974; Vol. 1, p 129.

(25) Liptay, W.; Wortmann, R.; Böhm, R.; Detzer, N. *Chem. Phys.* **1988**, *120*, 439.

(26) Liptay, W.; Wortmann, R.; Schaffrin, H.; Burkhard, O.; Reitinger, W.; Detzer, N. *Chem. Phys.* **1988**, *120*, 429.

(27) Köler, M.; Friedrich, J.; Fidy, J. *Biochim. Biophys. Acta* **1998**, *1386*, 255.

(28) Wortmann, R.; Elich, K.; Liptay, W. *Chem. Phys.* **1988**, *124*, 395.

(29) Born, M.; Wolf, E. *Principles of Optics*, 6th ed.; Pergamon Press: Oxford, U.K., 1980.

(30) Walz, T.; Jamieson, S. J.; Bowers, C. M.; Bullough, P. A.; Hunter, C. N. *J. Mol. Biol.* **1998**, *282*, 833.

(31) Papiz, M. Z.; Prince, S. M.; Howard, T. D.; Cogdell, R. J.; Isaacs, N. W. *J. Mol. Biol.* **2003**, *326*, 1523.

(32) McDermott, G.; Prince, S. M.; Freer, A. A.; Hawthornthwaite-Lawless, A. M.; Papiz, M. Z.; Cogdell, R. J.; Isaacs, N. W. *Nature* **1995**, *374*, 517.

(33) Yanagi, K.; Gardiner, A. T.; Cogdell, R. J.; Hashimoto, H. *Phys. Rev. B* **2004**, in press.

(34) Ferry, J. D. *Viscoelastic Properties of Polymers*, 3rd ed.; John Wiley & Sons: New York, 1980.

(35) Child, W. C.; Ferry, J. D. *J. Colloid Sci.* **1957**, *12*, 327.

(36) Shimizu, K.; Yano, O.; Wada, Y. *J. Polym. Sci.* **1973**, *11*, 1641.

(37) Brooks, C. L., III; Karplus, M.; Pettitt, B. M. *Proteins: A theoretical perspective of dynamics, structure, and thermodynamics*; John Wiley & Sons: New York, 1988.

(38) McCammon, J. A.; Harvey, S. C. *Dynamics of proteins and nucleic acids*; Cambridge University Press: Cambridge, U.K., 1987.

(39) Czarnecki, K.; Chynwat, V.; Erickson, J. P.; Frank, H. A.; Bocian, D. F. *J. Am. Chem. Soc.* **1997**, *119*, 2594.

(40) Czarnecki, K.; Diers, J.; Chynwat, V.; Erickson, J. P.; Frank, H. A.; Bocian, D. F. *J. Am. Chem. Soc.* **1997**, *119*, 415.

(41) Czarnecki, K.; Schenck, C. C.; Bocian, D. F. *Biochemistry* **1997**, *36*, 14697.